Effect of initial chirp on near-infrared supercontinuum generation by a nanosecond pulse in a nonlinear fiber amplifier*

Song Rui(宋 锐)[a], Hou Jing(侯 静)[a]†, Wang Ze-Feng(王泽锋)[a], Xiao Rui(肖 瑞)[b]‡, and Lu Qi-Sheng(陆启生)[a]

[a] College of Optoelectronic Science and Engineering, National University of Defense Technology, Changsha 410073, China
[b] Beijing Institute of Radiation Medicine, Beijing 100850, China

(Received 18 December 2012; revised manuscript received 26 March 2013)

Theoretical and experimental research on the effect of initial chirp on near-infrared supercontinuum generation by a nanosecond pulse in a nonlinear fiber amplifier is carried out. The complex Ginzburg–Landau equation is used to simulate the propagation of the pulse in the fiber amplifier and the results show that pulses with negative initial chirp produce the widest supercontinuum and pulses with positive initial chirp produce the narrowest supercontinuum when the central wavelength of the pump lies in the normal dispersion region of the gain fiber. A self-made line width narrowing system is utilized to control the initial chirp of the nanosecond pump pulse and a four-stage master oscillator power amplifier configuration is adopted to produce a high power near-infrared suppercontinuum. The experimental results are in good agreement with simulations which can provide some guidance on further optimization of the system in future work.

Keywords: fiber laser, supercontinuum, initial chirp, fiber amplifier

PACS: 42.55.Wd, 42.65.Tg **DOI:** 10.1088/1674-1056/22/8/084206

1. Introduction

The high power near-infrared supercontinuum (SC) has a wide range of applications such as spectroscopy,[1] real time optical metrology,[2] and chemical sensing.[3] Photonic crystal fiber (PCF) has been the dominant nonlinear medium in visible and near-infrared SC generation as a result of its flexible dispersion control and high nonlinearity.[4,5] However, many good results have been achieved using a fiber amplifier as the nonlinear medium in SC generation in recent years,[6–10] and the simple structure, low splicing loss, and high optical to optical conversion efficiency soon attracts the attention of many researchers. We have achieved a 70-W high power near-infrared SC with this method which proved its advantages in high power SC generation.[11]

A pulse's initial chirp has a significant effect on SC generation. Lots of experimental and numerical simulations were carried out to clarify the influence of initial chirp on SC generation by femtosecond or picosecond pulses in the normal or abnormal dispersion region of PCF with one or two zero-dispersion wavelengths, and the mechanisms behind the results were analyzed and some useful conclusions were obtained.[12–16] However, the effect of the initial chirp on near-infrared SC generation by a nanosecond pulse in a nonlinear fiber amplifier has been rarely reported which is different with that in PCF pumped by ultra-short pulses, and the initial chirp is also a key factor for the pulsed fiber laser seed in master oscillator power amplifier (MOPA) configuration. So it is of great necessity to carry out some theoretical and experimental research on it.

2. Ginzburg–Landau equation

The complex Ginzburg–Landau equation is used in this paper to describe the formation and propagation of near-infrared SC in the nonlinear fiber amplifier, which is shown below[17]

$$\begin{aligned}&\frac{\partial A}{\partial z}+\frac{\alpha}{2}A-\mathrm{i}\sum_{k\geq 1}\frac{\mathrm{i}^k\beta_k}{k!}\frac{\partial^k A}{\partial t^k}\\&=\mathrm{i}\gamma\left(1+\frac{\mathrm{i}}{\omega_0}\frac{\partial}{\partial t}\right)\cdot\left[A(z,t)\int_{-\infty}^{\infty}R(t')\cdot\left|A(z,t-t')\right|^2\mathrm{d}t'\right]\\&\quad+\frac{\mathrm{i}}{2}g_0L_\mathrm{d}\int_{-\infty}^{\infty}\frac{A(z,\omega)\exp(-\mathrm{i}ft)}{1+f/f_0-\mathrm{i}\left(f_0^2-f_\mathrm{a}^2+2ff_0\right)/f_\mathrm{a}\Delta f}\mathrm{d}f,\end{aligned}\quad(1)$$

where $A(z,t)$ is the slowly varying amplitude of the pulse envelope and $A(z,\omega)$ is the Fourier transformation of $A(z,t)$. α is the loss of the gain fiber, and β_k is the k-th order dispersion coefficient. γ is the nonlinearity parameter at the carrier frequency, $R(t)$ is the nonlinear response function. $L_\mathrm{d}=T_0^2/|\beta_2|$ is the dispersion length where T_0 is the width of the input pulse. g_0 is the time-dependent gain which can be described by

$$g_0(z,t)=g\exp\left[-\frac{1}{E_\mathrm{s}}\int_{-\infty}^{t}|A(z,t)|^2\,\mathrm{d}t\right],\quad(2)$$

*Project supported by the State Key Program of the National Natural Science Foundation of China (Grant No. 61235008), the National Natural Science Foundation of China (Grant Nos. 61077076, 11004247, and 11274385), the International Science & Technology Cooperation of China (Grant No.2012DFG11470), the Natural Science Foundation for Distinguished Young Scholars of Hunan Province of China (Grant No. 12JJ1010), the Outstanding Youth Fund Project of Hunan Province of China, and the Fund of Innovation of National University of Defense Technology of China (Grant No. B120701).

†Corresponding author. E-mail: houjing25@sina.com

‡Corresponding author. E-mail: ruixiao203@sina.com

© 2013 Chinese Physical Society and IOP Publishing Ltd

where E_s and g are the saturation energy and small signal gain coefficient of the ytterbium-doped fiber respectively. The shape and bandwidth of the gain spectrum are set Lorentz and 40 nm respectively with central wavelength at 1064 nm. One photon per mode noise model[18] and full Raman response model[19] are adopted in Eq. (1), and an adaptive split-step Fourier method is used to solve the complex Ginzburg–Landau equation.[20,21] Supposing the shape of the input pulse is Gaussian and the formula for a Gaussian pulse with initial chirp can be described as:

$$A(0,t) = \exp\left(-\frac{(1+\mathrm{i}C)}{2}\frac{t^2}{T_0^2}\right), \tag{3}$$

where C is the initial chirp of the input pulse, and the chirp is positive if $C > 0$ and negative if $C < 0$. The dispersion parameters of the gain fiber used in this paper are measured by a Mach–Zehnder interferometer,[22] and the dispersion parameters are list in Table 1.

Table 1. The dispersion parameters of the ytterbium-doped fiber.

Type of fiber	$\beta_2/(s^2/m)$	$\beta_3/(s^3/m)$	$\beta_4/(s^4/m)$	$\beta_5/(s^5/m)$	$\beta_6/(s^6/m)$
30/250 μm YDF	5.5934×10^{-26}	-3.3800×10^{-41}	7.4705×10^{-55}	2.8586×10^{-68}	-1.7555×10^{-82}

3. Simulation results

In order to save calculation time we set the shape, the pulse width, and the peak power of the input pulse to be Gaussian, 10 ps, and 10 kW, respectively. The diameter of the core and cladding of the ytterbium-doped fiber are 30 μm and 250 μm, respectively. The length of the gain fiber is 5 m and the small signal gain coefficient $g = 3.6/\mathrm{m}$. The nonlinearity parameter $\gamma = 0.0003864/\mathrm{W\cdot m}$. Figure 1 shows the simulation results when the initial chirp $C = 0$. The first-order and second-order Stokes occurred when the pulse propagates at $z = 2.2$ m and $z = 3$ m respectively. Some weak spectrums are produced near 1000 nm at $z = 2.8$ m, which result from the generate four-wave mixing (FWM) effect between the 1064-nm signal and the first-order Stokes light. The spectrum enters dramatic broadening stage when the pulse reaches at $z = 4.7$ m and around 400 nm new frequencies in the long wavelength direction are generated. The final output spectrum is shown in Fig. 1(b) which covers from 1000 nm to 1800 nm. However, the spectral components above the zero-dispersion wavelength of the gain fiber (around 1.3 μm) are quite weak and the spectral flatness is not good either. The reason is soliton-related nonlinear effects are weak such as soliton fission, soliton collisions, and soliton self-frequency shift (SSFS). Figures 1(c) and 1(d) describe the propagation of the pulse in the fiber amplifier in the time-domain and the final output single pulse shape respectively. The pulse width keeps increasing on the whole which is caused by the combined effects of dispersion and nonlinearity. Multi-peaks occurred when the pulse propagates at $z = 2$ m and the picosecond pulse is split into a series of femtosecond ultra-short pulses by modulation instability at $z = 4$ m. The femtosecond ultra-short pulses are within the envelope of the picosecond pulse and most femtosecond pulses lies in front part of the envelope. This is because the dispersion of the gain fiber is small compared with PCF and the pulse propagates in the normal dispersion region of the gain fiber for the majority of the whole time.

Figure 2 is the simulation result when the initial chirp $C = 3.8$ and other parameters keep unchanged. The occurrence of the stimulated Raman scattering (SRS) and generate FWM effects are similar with that in Fig. 1. However, the dramatic spectrum broadening phenomenon in Fig. 1(a) disappears in Fig. 2(a) as a result of the huge positive initial chirp. This is because the wavelength of the pump lies in the normal dispersion region of the gain fiber and dispersion as well as nonlinear effects like self-phase modulation (SPM) produces positive chirps to the pulse. The positive initial chirp accelerates the broadening of the pulse width and slows down the increase of the peak power compared with no initial chirp condition. So the pulse needs to propagate further in the fiber amplifier to reach the threshold of nonlinear effects and the occurrence of the dramatic spectrum broadening stage is postponed. As a result, the width of the final output spectrum in Fig. 2(b) is about 250-nm narrower than that in Fig. 1(b). Figures 2(c) and 2(d) are the time-domain propagation of the pulse in the fiber amplifier and the final single pulse output shape respectively, and there is no big difference from Figs. 1(c) and 1(d).

Figure 3 shows the simulation result when the initial chirp $C = -3.8$ and other parameters keep unchanged. The occurence of the nonlinear effects like SRS and FWM are similar to that in Fig. 2 and Fig. 1, but dramatic spectrum broadening phenomenon appears in Fig. 3(a) at $z = 4.5$ m, which is about 0.2-m earlier than that in Fig. 1(a) and demonstrating that a negative initial chirp is profitable in near-infrared SC generation. The negative initial chirp results in $\beta_2 C < 0$, and the chirps produced by dispersion and nonlinear effects like SPM are in opposite signs which can compensate for each other and result in a balance. As a result, the broadening factor for the pulse width is smaller compared with that in Fig. 1 and Fig. 2, and the peak power of the pulse increases faster which enhances the nonlinear effects and makes the dramatic spectrum broadening stage occurs earlier. So the width of the final output spectrum in Fig. 3(b) is a little wider than that in Fig. 1(b) and with better spectral flatness. Figures 3(c) and 3(d) describe the time-domain propagation of the pulse in the fiber amplifier and the final output single pulse shape respectively, which are quite similar to Fig. 1 and Fig. 2.

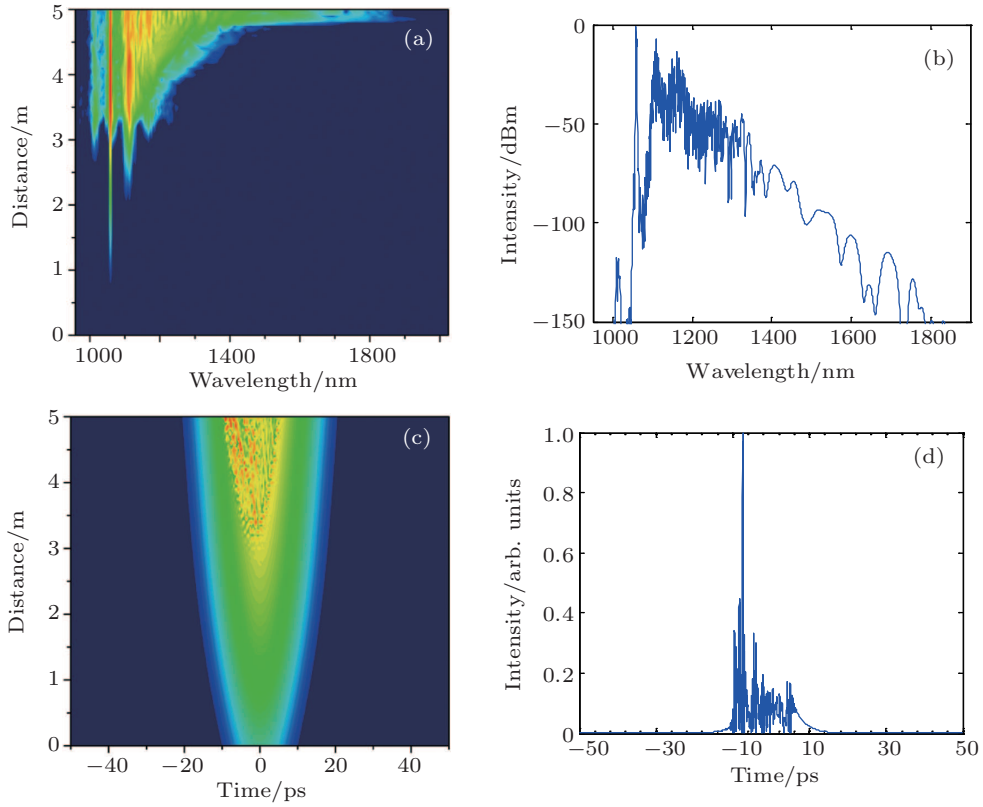


Fig. 1. (color online) Simulation results when $C = 0$, (a) frequency-domain propagation of the pulse in the fiber amplifier, (b) final output of the spectrum, (c) time-domain propagation of the pulse in the fiber amplifier, (d) final output of the pulse.

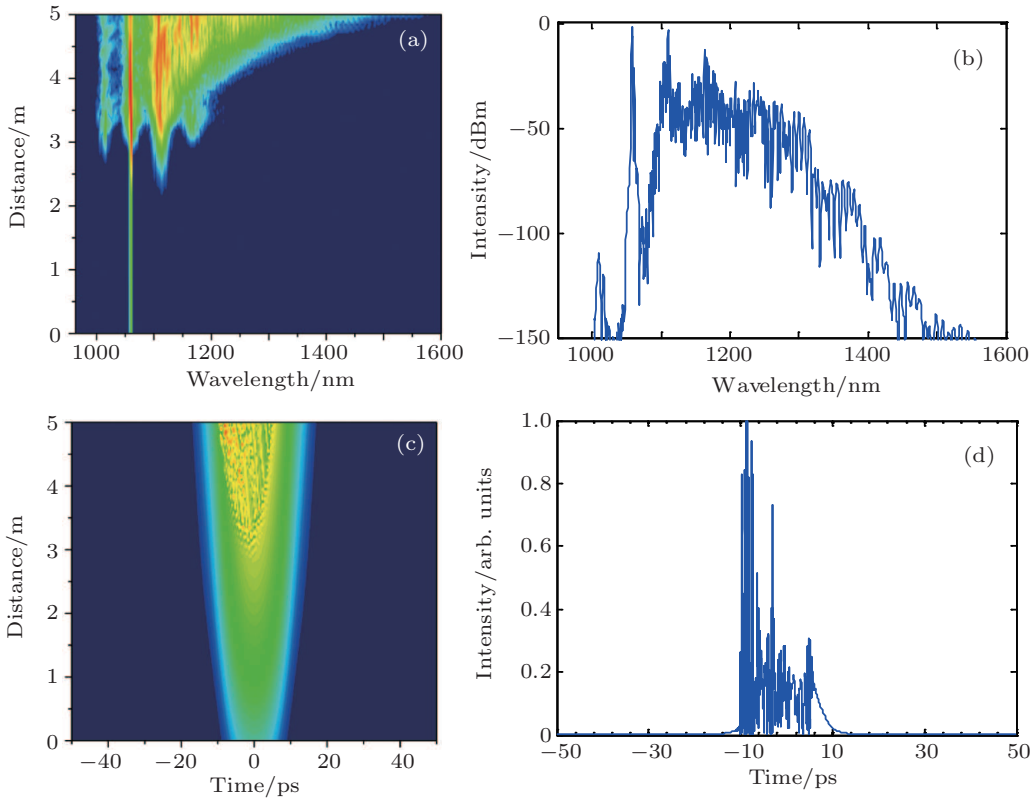


Fig. 2. (color online) Simulation results when $C = 3.8$, (a) frequency-domain propagation of the pulse in the fiber amplifier, (b) final output of the spectrum, (c) time-domain propagation of the pulse in the fiber amplifier, (d) final output of the pulse.

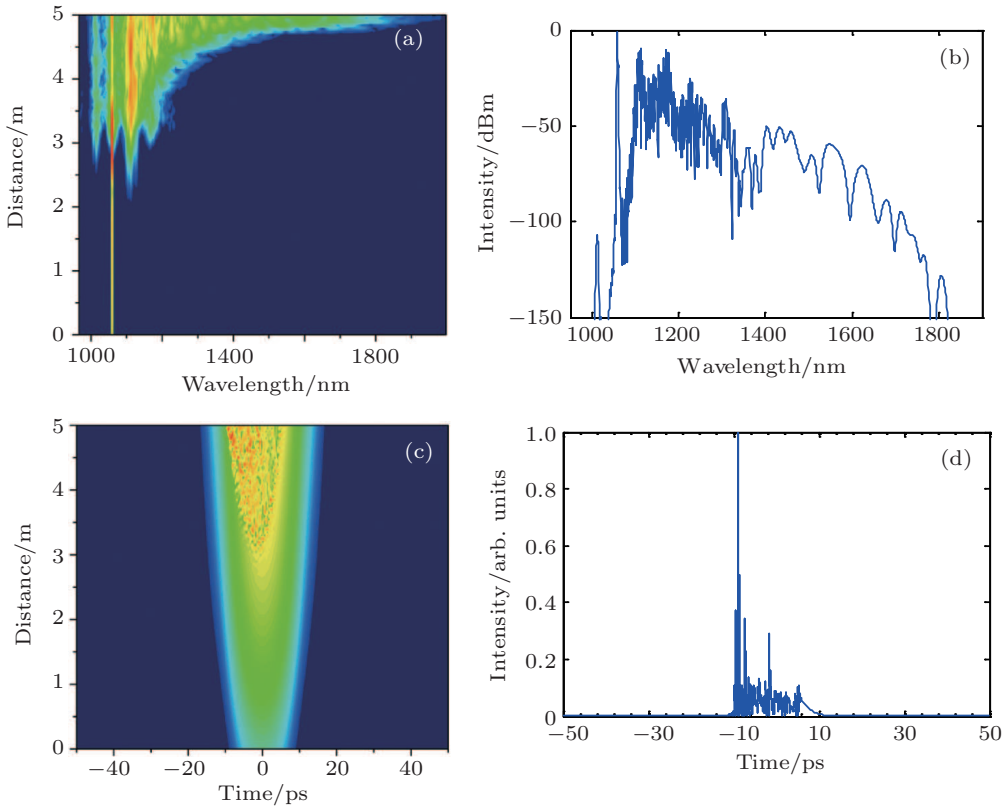


Fig. 3. (color online) Simulation results when $C = -3.8$, (a) frequency-domain propagation of the pulse in the fiber amplifier, (b) final output of the spectrum, (c) time-domain propagation of the pulse in the fiber amplifier, (d) final output of the pulse.

In a word, pulses with negative initial chirp results in the widest near-infrared SC and best spectral flatness compared with no initial chirp and positive initial chirp condition when the central wavelength of the pump pulse lies in the normal dispersion region of the gain fiber.

4. Experiments

In order to verify the above simulation results some relevant experiments are carried out and the experimental setup is shown in Fig. 4. The whole system is constructed in a four-stage master oscillator power amplifier (MOPA) configuration. The nanosecond fiber laser seed has been reported in Ref. [23], and the setup of the line width narrowing system has been described in Ref. [24] which is used to control the initial chirp of the nanosecond pulse. The second stage is a single mode ytterbium-doped fiber amplifier (YDFA) and both the third and fourth stages are double clad YDFA which have been described in detail in Ref. [11]. The output fiber end is angle polished to reduce back reflection and prevent end facet damage. A multimode large-core fiber (50 μm/125 μm) couples some output light into an oscilloscope (Tektronix, TDS7154) with 20-GHz sampling rate and a high speed photo detector (Thorlabs DET01CFC) and into an optical spectrum analyzer with 0.07-nm resolution (Agilent 86142B-E02) to analyze the time-domain and frequency-domain output of the system.

The function of the line width narrowing system is to control the initial positive chirp of the nanosecond pulse. We only compare the results between the pump pulse with large initial positive chirp and huge initial positive chirp because it is hard to construct a nanosecond fiber laser seed with negative or zero initial chirp. Figure 5 shows the output spectrum at different output power under nanosecond pump pulse with large initial positive chirp where $C = 890$. The spectrum broadening process and nonlinear effects involved are analyzed in detail in Ref. [11], which will not be discussed here again.

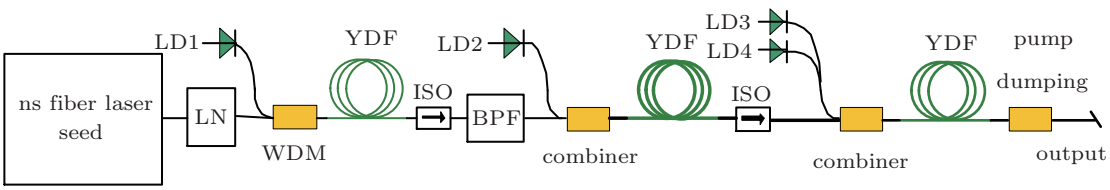


Fig. 4. (color online) High power SC generation from fiber amplifier in MOPA configuration, LN: line width narrowing system, YDF: ytterbium-doped fiber, ISO: isolator, BPF: bandpass filter, LD: laser diode.

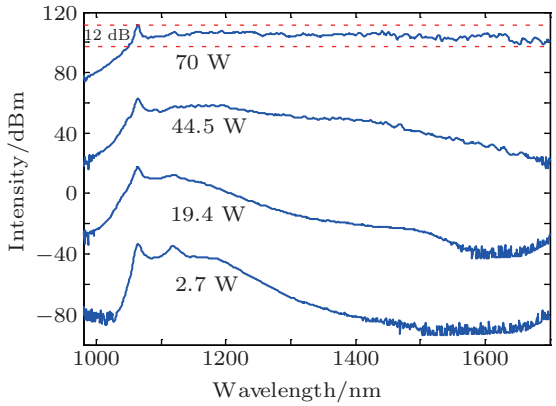


Fig. 5. (color online) Output spectrums at different output powers when $C = 890$.

Figure 6 shows the output spectrums at different output powers under a nanosecond pump pulse with huge initial positive chirp where $C = 8900$. These four output spectrums are under the same pump power compared with that in Fig. 5. However, the average output powers are a little higher and the flatness of the spectrums is not so good. The central wavelength of the small spectral peak on the left side of 1064-nm peak is 1030 nm when the average output power is 76.5 W, which means the input signal power of the last stage fiber amplifier is not strong enough. The results demonstrating that pulses with huge initial positive chirp slows down the increase of the peak power and reduces the conversion efficiency of the SRS effect, which makes most 976-nm pump changed into 1064-nm signal light and the spectrum intensity in the long wavelength direction is weak. As a result, soliton related nonlinear effects like soliton fission, soliton collisions, and SSFS could not effectively produce new frequencies in the abnormal dispersion region of the gain fiber.

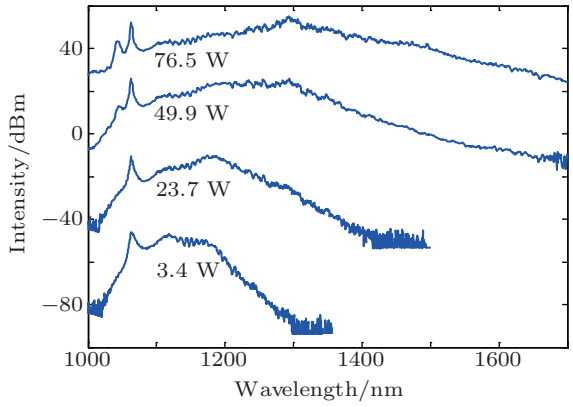


Fig. 6. (color online) Output spectrums at different output power, when $C = 8900$.

Figures 7(a) and 7(b) are the time-domain final output of the pulse train and single pulse shape respectively. The line width narrowing system has no effect on the time-domain output. The output pulse train still keeps the same repetition rate with the nanosecond fiber laser seed, and the complex multi-peak structure in the middle of the pulse in Fig. 7(b) is caused by the overlap of the femtosecond ultra-short pulses. The experimental results are in good agreement with simulations. In addition, the experimental results in Refs. [25] and [26] are also in good accordance with the simulations in terms of the change between the spectrum and the pump power, which verified the feasibility of the model that we used in this paper.

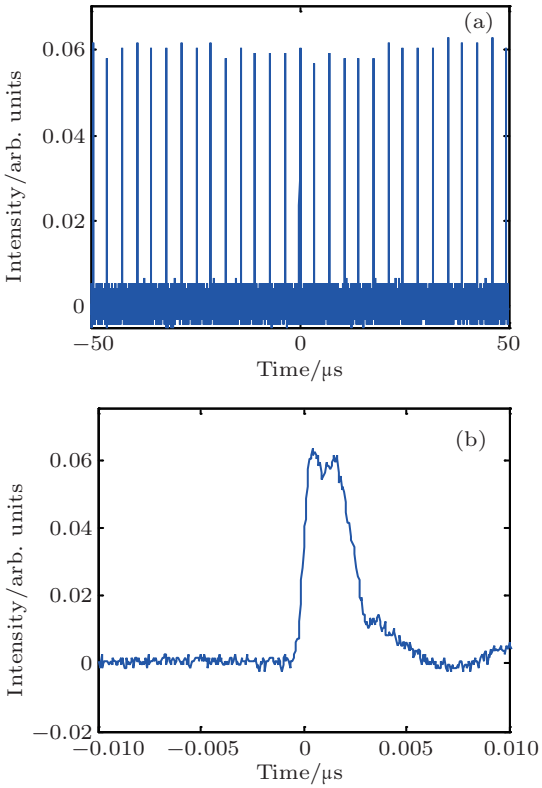


Fig. 7. (color online) Time-domain output at maximum output power, (a) pulse train, (b) single pulse shape.

5. Conclusion

The effects of initial chirp on near-infrared SC generation by a nanosecond pulse in a nonlinear fiber amplifier are studied both theoretically and experimentally. The complex Ginzburg–Landau equation is used to simulate the propagation of the pulse in the fiber amplifier and the results show that a negative initial chirp is most profitable in near-infrared SC generation. The initial chirp control of the nanosecond fiber laser seed is realized by a self-made line width narrowing system, and four-stages MOPA configuration is adopted to produce high power near-infrared SC. The experimental results between nanosecond pulses with large positive initial chirp and huge positive initial chirp are compared with each other which are in good agreement with simulations. This paper may shed some light on further optimization of the width and flatness of the output near-infrared SC in future work.

References

[1] Kumar M, Islam M N F L T Jr, Freeman M J, Chan A, Neelakandan M and Manzur T 2012 *Appl. Opt.* **51** 2794

[2] Diddams S A, Jones D J, Ye J, Cundiff S T, Hall J L, Ranka J K, Windeler R S, Holzwarth R, Udem T and Hänsch T W 2000 *Phys. Rev. Lett.* **84** 5102
[3] Mandon J, Sorokin E, Sorokina I T, Guelachvili G and Picqué N 2008 *Opt. Lett.* **33** 285
[4] Russell P 2003 *Science* **299** 358
[5] Knight J C 2003 *Nature* **424** 847
[6] Zhang B, Hou J, Liu P Z, Jin A J and Jiang Z F 2011 *Laser Phys.* **21** 1895
[7] Roy A, Leproux P, Roy P, Auguste J L and Couderc V 2007 *J. Opt. Soc. Am. B* **24** 788
[8] Pioger P H, Couderc V, Leproux P and Champert P A 2007 *Opt. Express* **15** 11358
[9] Kurkov A S, Kamynin V A, Sholokhov E M and Marakulin A V 2011 *Laser Phys. Lett.* **8** 754
[10] Geng J, Wang Q and Jiang S 2012 *Appl. Opt.* **51** 834
[11] Song R, Hou J, Chen S, Yang W Q and Lu Q S 2012 *Opt. Lett.* **37** 1529
[12] Driben R and Zhavoronkov N 2010 *Opt. Express* **18** 16733
[13] Zhu Z and Brown T 2004 *Opt. Express* **12** 689
[14] Zhang H, Yu S, Zhang J and Gu W 2007 *Opt. Express* **15** 1147
[15] Jiang Y, Zhou B, Leng Y, Liang X and Xu Z 2007 *Chin. Opt. Lett.* **5** S229
[16] Hu X, Wang Y, Zhao W, Yang Z, Zhang W, Li C and Wang H 2010 *Appl. Opt.* **49** 4984
[17] Agrawal G P 2008 *Applications of Nonlinear Fiber Optics*, 4th edn. (Burlington: Academic Press) p. 503
[18] Kobtsev S and Smirnov S 2005 *Opt. Express* **13** 6912
[19] Erkintalo M, Genty G, Wetzel B and Dudley J M 2010 *Opt. Express* **18** 25449
[20] Sinkin O V, Holzlöhner R, Zweck J and Menyuk C R 2003 *J. Lightwave Technol.* **1** 61
[21] Liu X and Lee B 2003 *Photon. Technol. Lett.* **15** 1549
[22] Jin A, Wang Z, Hou J, Zhang B and Jiang Z F 2011 *Proceedings of* 2011 *International Conference on Electronics and Optoelectronics*, July 29, 2011, Dalian, China, p. 181
[23] Song R, Chen H W, Chen S P, Hou J and Lu Q S 2011 *J. Opt.* **13** 35201
[24] Song R, Chen S, Hou J and Lu Q S 2011 *Proceedings of* 2011 *International Conference on Electronics and Optoelectronics* July 29, 2011, Dalian, China, p. 116
[25] Liu X M, Wang L R, Mao D and Duan L N 2012 *Laser Phys.* **22** 227
[26] Duan L N, Liu X M, Wang L R, Mao D and Wang G X 2011 *Laser Phys.* **21** 1813